Fundamental Study of the Dissolution of Calcium Phosphonates from Porous Media

F. Henry Browning and H. Scott Fogler
Dept. of Chemical Engineering, The University of Michigan, Ann Arbor, MI 48109

Phosphonate-scale inhibitors are commonly used to prevent scale formation in many industrial processes involving high-salinity brine solutions. To effectively prevent scale formation in these industrial processes, one must have a fundamental understanding of how phosphonates are released into high-salinity brines. Because phosphonates can precipitate with divalent cations such as calcium, their release into aqueous media is often governed by many dissolution mechanisms. This study focuses on the release of calcium-phosphonate precipitates from porous media (as related to oil-field applications) and a mathematical model describing these release mechanisms based on mechanistic studies of pore-level phenomena. The phosphonate used was 1-hydroxyethylidene-1,1-diphosphonic acid (HEDP). The release of two distinct calcium-HEDP precipitates from porous media was studied: soluble, fibrous 1:1; insoluble, spherical 2:1. Visual studies using etched-glass micromodels showed that five distinct regimes govern the release of 1:1 calcium-HEDP precipitate from porous media. Conversely, the release of 2:1 calcium-HEDP precipitate was dominated by two distinct regimes. A continuum model developed describes the release of both precipitates from porous media by mathematically describing each of the distinct release regimes and defining conditions under which the transition between release regimes occurred. Experimental data agreed excellently with model simulations for both precipitates.

Introduction

The use of phosphonates as threshold-scale inhibitors to prevent undesirable precipitation (scale) is commonly encountered in many facets of industry where high-salinity brines are present (Kan et al., 1994; Monsanto, 1986). Some of the more pronounced phosphonate applications are found in such places as cooling water towers, boiler water systems, paper mills, and petroleum production systems (Monsanto, 1986a,b). Phosphonates are advantageous in scale-prevention treatments because they have the ability to slow or prevent scale-nucleation/crystal-growth processes and are stable over a wide range of conditions such as temperatures and pressures (Kan et al., 1994; Mohanty et al., 1990; Estrin, 1990; Nancollas, 1979; Walton, 1967; Hach, 1980). In addition to scale inhibition, phosphonates are effectively utilized in many industrial processes as dispersants, bleaching agents, or corrosion inhibitors (Monsanto, 1986a,b).

The treatment of high-salinity waters with phosphonates can potentially result in the precipitation of phosphonates with divalent cations such as calcium. This phenomenon is highly visible in oil-field applications when phosphonates are injected into the subsurface porous media and are left to interact with cation-containing formation waters for approximately 24 hours. Following this shut-in period, oil production is resumed and the divalent cation-phosphonate precipitates are redissolved into the produced fluid where the phosphonate is able to slow or completely prevent scale formation. This procedure is commonly referred to as a precipitation "squeeze" treatment. Once the phosphonate has been exhausted from the rock formation, production is discontinued and the squeeze treatment has to be reapplied to the well which, in turn, is costly to producers in terms of chemicals and production downtime. Hence, it is imperative for oil producers to perform squeeze treatments that maximize treat ment lifetimes, thereby minimizing costs. Previous research has shown that the precipitation and subsequent dissolution

Correspondence concerning this article should be addressed to H. S. Fogler.

of divalent cation-phosphonate precipitates from porous media enhance treatment lifetimes by increasing the amount of phosphonate retention during the shut-in period and slowing the release characteristics of phosphonates into produced fluids during production (Carlberg, 1987; Berkshire et al., 1982; Ciba-Geigy, 1989). Because the success of a phosphonate treatment is often measured by its resulting lifetime (in oilfield applications, as well as in other industrial applications), the design of efficient phosphonate treatments in oil fields requires a fundamental understanding of the precipitation/dissolution mechanisms of phosphonates in porous media (which, in the past, has not been readily available). A mathematical model describing the release of phosphonates from a porous medium will help enhance the fundamental understanding of these processes and can be used to improve the design of future squeeze treatments. Similarly, a model of this sort could be extended to describe the governing phosphonate release mechanisms in other industrial processes that employ similar phosphonate treatment procedures, for example, cooling water towers.

Given the importance of phosphonates and their precipitates as treatment chemicals in industrial operations involving high-salinity brines, it is surprising to note that relatively few mathematical models have been developed to describe the release of phosphonate precipitates into an aqueous medium following standard injection procedures. Various continuum and network models have been developed to successfully describe precipitate dissolution in porous media (Walsh et al., 1984; Hoefner and Fogler, 1988; Rege and Fogler, 1989). Existing models developed with respect to oilfield applications consist of continuum models or simulators where the dissolution of phosphonate precipitates is assumed to be governed by a nonequilibrium process driven by the concentration difference between that in the produced fluid and that at the solubility limit. The elution-curve simulations are then empirically matched to experimental or field data using fitting parameters while the effects of different treatment parameters on the treatment performance are examined (Atkinson et al., 1993; Yuan et al., 1992). A more sophisticated two-phase, two-dimensional simulator has been developed to account for radial effects and produced fluid crossflow, although the dissolution process itself is analogous to other models (Yuan et al., 1992). These simulators are extremely useful tools in analyzing precipitation squeeze treatments and in understanding the effects that squeeze parameters (inhibitor concentration, overflush volume, etc.) have on the treatment performance. However, to complement these simulators, mathematical models that provide a more fundamental, pore-level approach to describe the release of precipitate from a precipitation squeeze need to be developed in an effort to better understand and more accurately simulate the distinct dissolution regimes governing the phosphonate release process. Hence, the objective of this work is *to develop a mathematical model based on mechanistic studies of pore-level phenomena that describes the release of calcium-phosphonate precipitates from porous media*. This model will help provide the fundamental understanding necessary to design effective squeeze treatments based on science rather than just on experience. More specifically, this model can be used to improve future squeeze treatments by elucidating the factors that dominate the release of phosphonates from porous media and by predicting how changing conditions affect these factors and the resulting squeeze lifetimes. Although the modeling in this article will be specific to the calcium-phosphonate precipitates under study, the basic shape of most precipitate elution curves is similar and the general structure of this model can be applied to describe the release of many different precipitates from porous media with some modification. In addition, this model can be extended to describe the governing phosphonate release mechanisms in other industrial processes that employ similar phosphonate treatment procedures.

Release of Calcium-Phosphonate Precipitates from Porous Media

After injection of phosphonate into a formation, the phosphonate can react with divalent cations (most notably calcium) to form calcium-phosphonate precipitates. Once production is resumed following the reaction shut-in period, the mechanism by which the calcium-phosphonate precipitate is released back into the produced fluid governs the rate of phosphonate release and hence, the squeeze treatment lifetime. Following a precipitation squeeze, a characteristic elution curve can be obtained by monitoring the concentration of phosphonate in the produced fluid as a function of time (or fluid flow). A typical elution curve resulting from a precipitation squeeze treatment is depicted in Figure 1. Five distinct regions of the elution curve have been identified: (1) an initial flat region; (2) a sharp declining region; (3) a more gradually declining region; (4) a long tailing region; and (5) a final sharp declining region. It should be noted that five different regions may not exist for all calcium-phosphonate precipitates (as we will see later with an alternative precipitate), but the general shapes are similar. With the characteristic shape of an elution curve being determined by the rate at which the phosphonate is released from porous media, it becomes evident that the dissolution regimes governing the re-

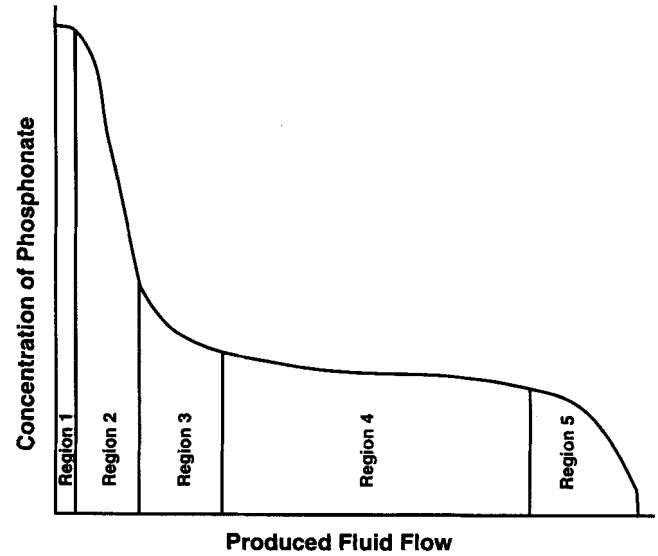

Figure 1. Breakdown of a typical elution curve resulting from the dissolution of a 1:1 calcium-HEDP precipitate in porous media.

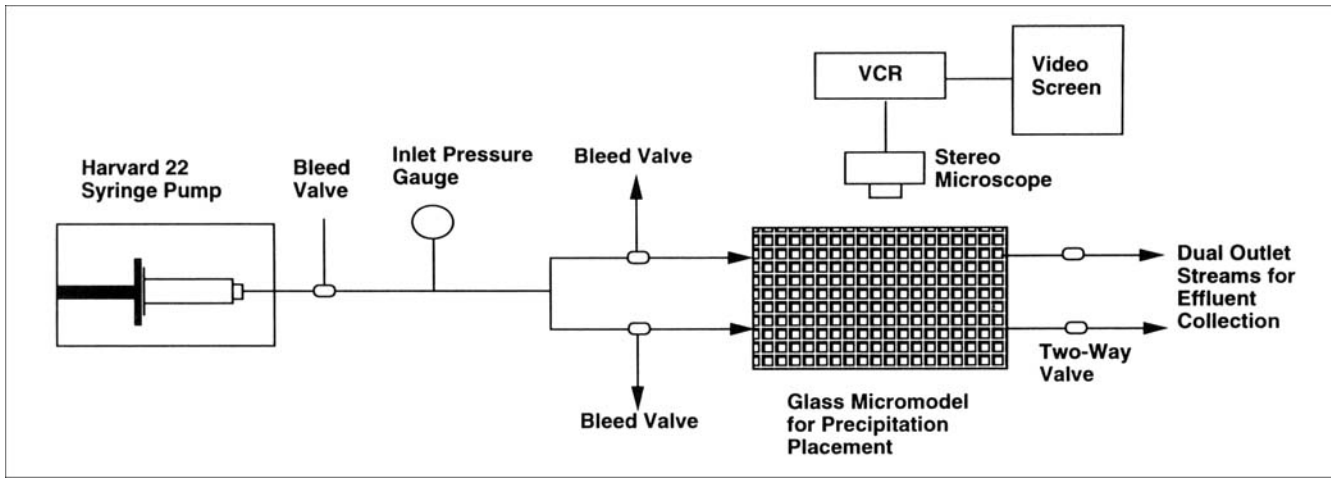

Figure 2. Apparatus used to perform micromodel experiments.

lease of calcium-phosphonate precipitates change during the course of the elution process. Therefore, to accurately model the release process and predict squeeze lifetimes from precipitation squeeze treatments, it becomes extremely important to have a fundamental understanding of each dissolution regime and the factors that affect the release of calcium-phosphonate precipitates during these regimes.

The use of etched-glass micromodels to simulate porous media has provided valuable insight into understanding each dissolution regime that occurs during the release of calcium-phosphonate precipitates. Micromodel experiments have the advantage that through the use of a stereo zoom microscope and a VCR, the precipitate placement and subsequent release processes can be visually observed and recorded. The micromodels themselves offer an idealistic but insightful representation of actual porous media in that they are two-dimensional (pore volume ~ 0.05 cm^3), contain well-defined pore bodies and pore throats (see Figure 3), and have relatively clean, nonreactive surfaces, that is, have no dissolving minerals such as carbonates. However, with their surfaces made of silicon dioxide (which is similar in composition to those seen in sandstone porous media), experimental work has shown that the micromodel elution curves closely resemble those found in consolidated porous media and the visual observations and trends seen in micromodels readily support results obtained in consolidated media (Browning and Fogler, 1995a). The apparatus used to perform micromodel experiments is illustrated in Figure 2. Time-lapse photographs depicting the sequential release of a calcium-phosphonate precipitate from a micromodel are shown in Figure 3 (Browning and Fogler, 1995b). In this particular experiment, calcium was mixed with 1-hydroxyethylidene-1,1-diphosphonic acid (HEDP, a commonly used phosphonate containing two phosphate groups) in a micromodel where precipitation was allowed to occur *in situ*. The resulting precipitate consisted of fiberlike spindles compacted into pore throats with long fibers extending outward into the pores' bodies (see Figure 3a). The micromodel was then eluted with deionized water (to simulate the produced fluid flow), and the release process of the calcium-HEDP precipitate was recorded. Comparing the time-lapse photographs in Figure 3, along with other similar experimental results, with the resulting elution curves made it possible to identify the *dominant* phosphonate release regime in each region of the elution curve as described below (Browning and Fogler, 1995b):

Region 1. Elution of saturated calcium-HEDP solution in contact with the precipitate, along with loose fibers not held in the media (~ 1–2 pore volumes).

Region 2. "External" hydrodynamic dissolution of the fibers extending outward into the pores. In this regime, the rate of dissolution is strongly affected by the hydrodynamics of flow around the fibers.

Region 3. "External/Internal" hydrodynamic dissolution of the densely packed precipitate in contact with the free-flowing fluid. In this regime, the rate of dissolution is also governed by hydrodynamics.

Region 4. Diffusion-controlled dissolution (from the precipitate–fluid interface to the pore-throat entrance) of the densely packed precipitate regions, referred to as pore-throat plugs, contained completely within the pore throats. This regime is not governed by the fluid hydrodynamics.

Region 5. Breaking and migration of the densely packed precipitation regions from the pore throats.

To gain a clearer understanding of how the sequential releases of the aforementioned calcium-HEDP precipitate occurs in porous media, an illustration of how each portion of a precipitate site contributes to each different region of the elution curve is shown in Figure 4.

A mathematical model to describe the release of this calcium-HEDP precipitate from porous media must account for the release regime occurring in each region of the elution curve. Models describing the release of other phosphonate precipitates from porous media must also be developed in a similar manner. This article focuses on modeling the release of two distinct calcium-HEDP precipitates from a porous medium, a calcium-HEDP precipitate having a molar composition of 1:1 (shown previously) and a calcium-HEDP precipitate with a 2:1 molar ratio. The model is based on mechanistic studies of pore-level phenomena dictating the sequential release regimes of calcium-phosphonates as described earlier. Although these modeling efforts are specific to the calcium-phosphonate precipitates under study, the basic shape

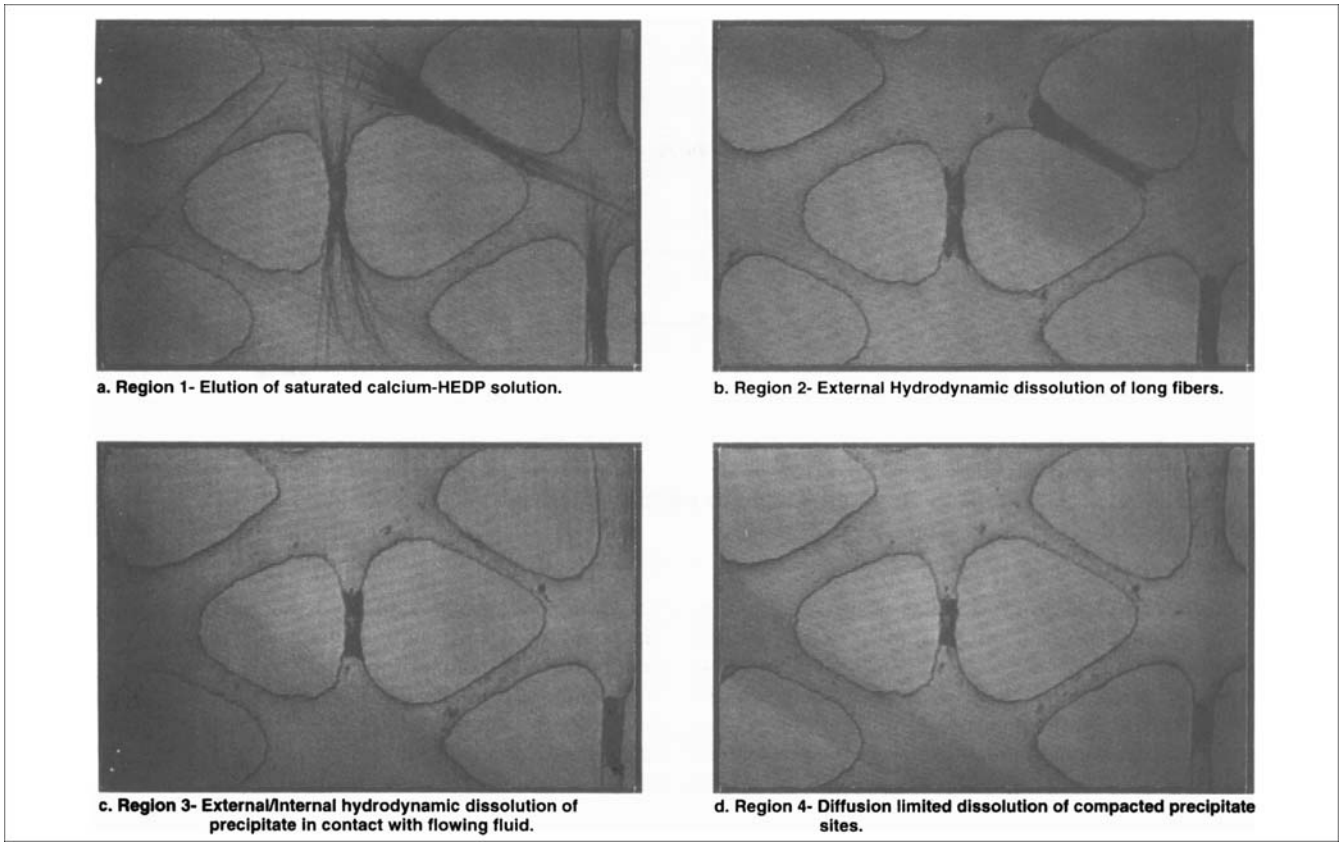

Figure 3. Different release regimes of 1:1 calcium-HEDP precipitate from a micromodel.

of most elution curves is similar and the general structure of this model can be applied to study the release mechanisms of other precipitates from porous media. Successful modeling will, in turn, enhance the design of efficient squeeze treatments and provide added insight to the factors dictating the release of calcium-phosphonate from porous media.

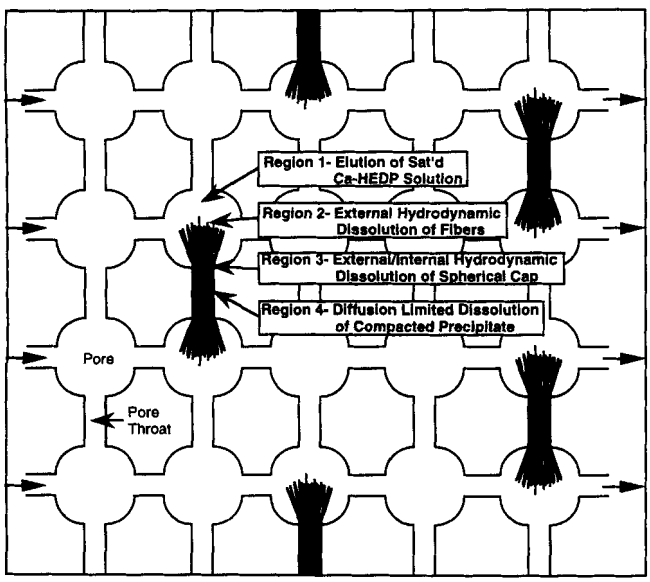

Figure 4. Illustration of how each section of a precipitate site is released from porous media. The basis for modeling the release of a 1:1 calcium-HEDP precipitate from porous media.

Description of the 1:1 Calcium-HEDP Release Model

The continuum model developed to describe the release of 1:1 calcium-HEDP precipitate from porous media is based upon the pore-level mechanisms observed in micromodel experiments described earlier. The physical situation that provides the basis for the model is illustrated in Figure 4. Identical precipitate sites, comprising tightly packed fibrous spindles situated in pore throats with n (number of fibers) long fibers extending outward into the pores, are assumed to uniformly decorate the porous media by assigning a site density (N/V, number of precipitate sites/pore volume of porous media) to the porous media reaction volume under study. This precipitate site placement strategy is analogous to the physical situation seen in micromodel experiments with the modification that the loose precipitate sites existing solely in pore bodies are neglected.

After the shut-in period, the fluid in contact with the precipitate sites is a saturated calcium-HEDP solution at the precipitating conditions. Flow of the elution fluid is initiated at a constant flow rate through one side of the porous media where it comes into contact with the precipitate sites and begins to dissolve these sites. The effluent concentration from the porous media is determined as a function of time, and an elution curve can be generated. To mathematically simulate

the release process of calcium-HEDP precipitate throughout the elution and account for the changing dissolution regimes, we must look more closely at the governing release mechanisms during each region of the elution curve and derive mathematical expressions to describe each mechanism.

Mathematical Expressions Describing the Five Release Regimes

To accurately model the release of HEDP from porous media following precipitate placement, the release in each regime must be described mathematically. The first regime is simply the displacement of the saturated calcium-HEDP solution in contact with the precipitate from the micromodel. The fifth regime, the breaking and migration of the compacted precipitate sites, requires an empirical analysis rather than a mathematical analysis that can be obtained by evaluating various micromodel experiments. The other three regimes, however, can be modeled mathematically to accurately predict the release of HEDP from porous media.

For each of the three dissolution regimes under study, the phosphonate concentration is mathematically determined as a function of time and length in the porous medium. To arrive at these desired expressions, a shrinking-core analysis, using appropriate mass-transfer correlations, was performed on each of the respective geometries to obtain the surface area as a function of time. In the case of the diffusion-controlled dissolution from the precipitate–fluid interface to the free-flowing fluid, the surface area was constant and the diffusion length was determined as a function of time. The shrinking-core analysis in each regime was performed assuming that the concentration driving force for dissolution ($C_s - C$), was not a strong function of length, which was ensured by discretizing the porous media. When the appropriate time-dependent expression obtained from the shrinking-core analysis is coupled with the mole balance for the ith reaction regime (neglecting dispersion),

$$\frac{\partial C}{\partial t} + v\frac{\partial C}{\partial z} = ar_i'', \tag{1}$$

and the reaction-rate law governing the ith regime,

$$r_i'' = k_i(C_s - C), \tag{2}$$

the method of characteristics can be used to obtain the desired concentration profiles as a function of time and length in each regime (Rhee et al., 1986). A more complete description of how the concentration profiles in each regime were solved is given below.

External hydrodynamic dissolution regime

The external hydrodynamic dissolution dominates the release of HEDP from the long fibers that extend outward into the pore bodies. The physical geometry of dissolution of an individual fiber is shown in Figure 5. To obtain the surface area of n fibers as a function of time for this geometry, the appropriate mass-transfer correlation (Bird et al., 1960),

$$k_m = 0.40\left(\frac{v}{r}\right)^{1/2}\left(\frac{D^{2/3}}{\nu^{1/6}}\right) \tag{3}$$

is combined with the mass balance of a single spindle,

$$r_m'' = k_m(C_s - C) = -\rho\frac{dr}{dt} \tag{4}$$

to arrive at the equation that gives the surface area of one precipitate site (containing n spindles) as a function of time,

$$a(t) = 2fn\pi L(r_o^{3/2} - \alpha t)^{2/3} \tag{5}$$

where L is the entire length of the fiber (in the pore body and pore throat), f is the fraction of fiber subject to hydrodynamic dissolution, and α is a lumped constant containing experimental parameters. Finally, Eqs. 1, 2 and 5 are combined and solved using the method of characteristics to give the concentration in this regime, C, as a function of time, t, and length, z, in a porous medium,

$$\frac{C_s - C_o}{C_s - C} = \exp\left\{\frac{-3\beta}{4\alpha}\left[(r_o^{3/2} - \alpha t)^{4/3} - \left[r_o^{3/2} - \alpha\left(t - \frac{z}{v}\right)\right]^{4/3}\right]\right\}, \tag{6}$$

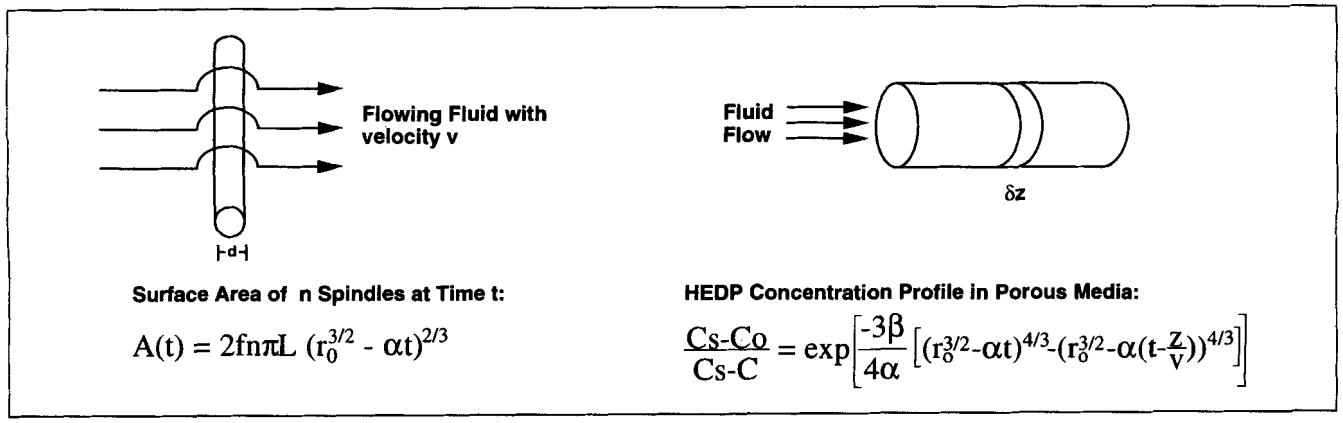

Figure 5. Physical geometry and mathematical expressions governing the hydrodynamic dissolution of long fibers.

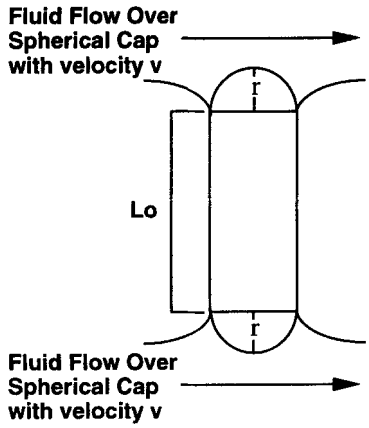

Surface Area for Dissolution Over Cap:

$$S.A. = 2\pi r^2$$

Definition of Mass Transfer Coefficient:

$$\frac{k_s d}{D} = 2.0 + \left(\frac{dv}{v}\right)^{1/2}\left(\frac{v}{D}\right)^{1/3}$$

Figure 6. Physical geometry and mathematical expressions governing the hydrodynamic dissolution of a spherical cap.

where β is a lumped constant containing the parameters N/V, L, and f. A summary of the governing equations is given in Figure 5.

External/internal hydrodynamic dissolution regime

The second dissolution regime, the external/internal hydrodynamic dissolution regime, starts when the fibers extending into the pore bodies have dissolved. The precipitate dissolving in this regime extends slightly past the pore-throat entrance and is still subject to the fluid hydrodynamics (velocity) over the dissolving surface (see Figures 3 and 4). The geometry of this portion of precipitate was modeled as a spherical cap, as illustrated in Figure 6. The mass-transfer coefficient to describe the dissolution in this regime is defined by the following equation (Cussler, 1993):

$$\frac{k_s d}{D} = 2 + 0.6\left(\frac{dv}{\nu}\right)^{1/2}\left(\frac{\nu}{D}\right)^{1/3}, \tag{7}$$

where the characteristic length, d, is assumed to be approximately equal to the pore-throat radius. Analogous to the procedure in the previous regime, Eq. 7 is coupled with the mole balance over the porous media and the rate law to obtain the concentration profile as a function of time and position,

$$\frac{C_s - C_o}{C_s - C} = \exp\left\{\frac{-2\beta}{3\alpha}\left[(r_o^2 - \alpha t)^{3/2} - \left[r_o^2 - \alpha\left(t - \frac{z}{v}\right)\right]^{3/2}\right]\right\}, \tag{8}$$

where α and β are lumped constants containing experimentally determined parameters such as k_s, N/V, and ρ.

Diffusion-limited dissolution regime

The diffusion-limited dissolution regime begins when the compacted precipitate sites have receded to the point where the hydrodynamic boundary layer is no longer important. Instead, the release of HEDP is limited by the rate of diffusion from the precipitate–fluid interface to the flowing fluid in neighboring pore bodies and pore throats. The physical flow geometry for this regime is shown in Figure 7. The mass-transfer coefficient in the diffusion-limited regime is a function of the diffusion length,

$$k_d = \frac{2D}{L_{pt} - l}. \tag{9}$$

Equation 9 can be coupled with the mass balance of a single compaction region,

$$r_d'' = k_d(C_s - C) = -\frac{\rho}{2}\frac{dl}{dt} \tag{10}$$

to arrive at the expression describing the site length as a function of time,

$$l = L_{pt} - \sqrt{\alpha_1 t + (L_{pt} - L_o)^2} \tag{11}$$

where α_1 is a lumped constant containing the parameters k_d, ρ, and D. The reaction surface area for a site in this regime is constant. In a manner similar to that in previous regimes, Eqs. 1, 9 and 11 can be combined and solved by the method of characteristics to obtain the desired concentration profile,

$$\frac{C_s - C_o}{C_s - C} = \exp\left\{\frac{2\beta_1}{3\alpha_1}\left[\left[(L_{pt} - L_0)^2 + \alpha_1 t\right]^{1/2} - \left[(L_{pt} - L_0)^2 + \alpha_1\left(t - \frac{z}{v}\right)\right]^{1/2}\right]\right\}, \tag{12}$$

where β_1 is a lumped constant containing the parameters N/V and n.

Equations 8 and 12 represent the concentration profiles for HEDP dissolution in the external/internal hydrodynamic and diffusion-controlled dissolution regimes, respectively. However, experimental results indicated that the dissolution of calcium-HEDP in these two regimes occurs in series. Hence, the two regimes were coupled and the mathematical expressions were solved simultaneously, as described in the next section.

Coupled diffusion-limited/hydrodynamic-dissolution regime

A physical description of this coupled regime is shown in Figure 8. In this regime, the size of the spherical cap is de-

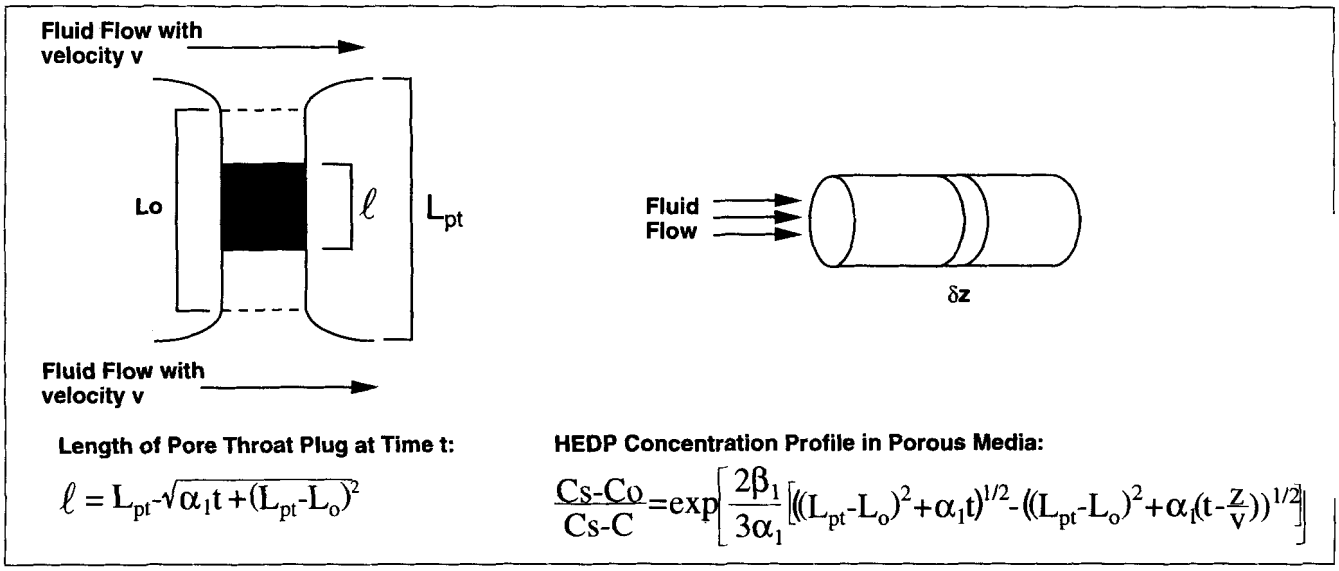

Figure 7. Physical geometry and mathematical expressions governing the diffusion-limited dissolution of a compacted precipitate site.

creasing while the compacted site itself is receding inward toward the center of the pore throat. Because the mass transfer of HEDP from the precipitate–fluid interface to the free-flowing fluid occurs in series, the total mass-transfer coefficient can be determined from the following relationship,

$$\frac{1}{k_t}=\frac{1}{k_s}+\frac{1}{k_d}, \tag{13}$$

where k_s will remain constant over the reaction time step if the radius of the spherical cap does not change appreciably, that is, if small time steps are chosen. Hence, a mass balance over the precipitate becomes,

$$k_t(C_s-C)=-\frac{\rho}{2}\frac{dl}{dt}=\frac{2Dk_s}{2D+k_s(L_{pt}-l)}(C_s-C). \tag{14}$$

Solving Eq. 14 yields the length of the compacted region as a function of time,

$$l=\frac{2D}{k_s}+L_{pt}-\sqrt{\left((L_{pt}-L_o)+\frac{2D}{k_s}\right)^2-\frac{2\alpha_2 t}{k_s}}, \tag{15}$$

where α_2 is a lumped parameter containing D, k_s, and ρ. By combining Eqs. 1, 14 and 15 and solving using the method of

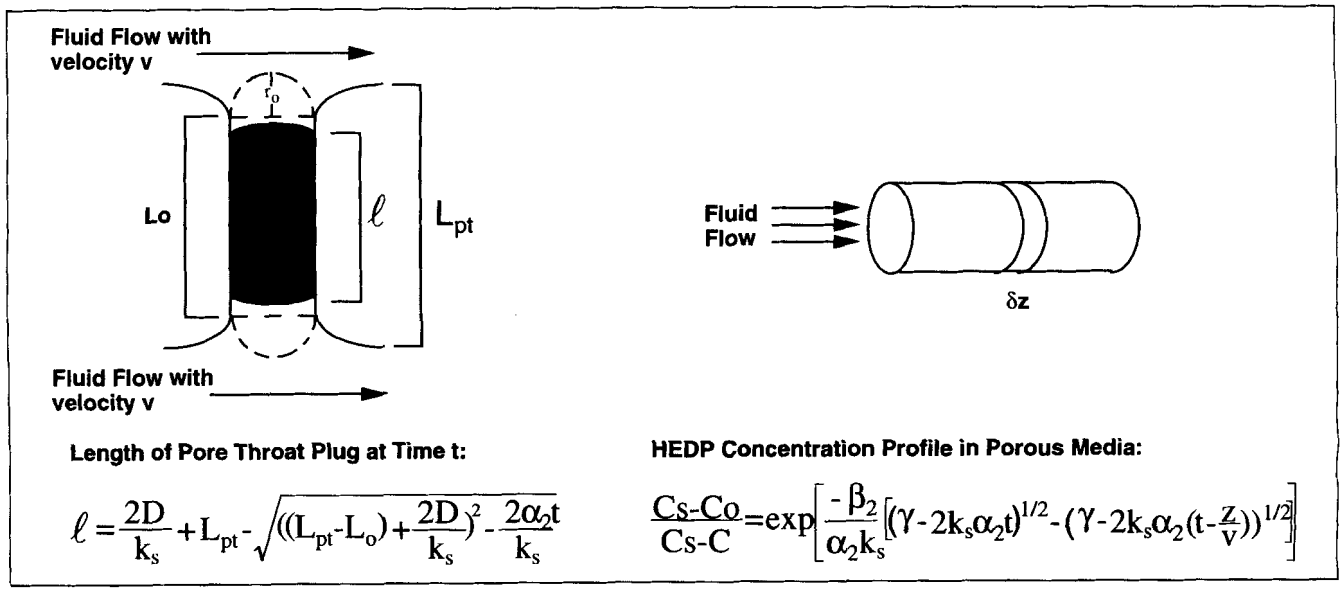

Figure 8. Physical geometry and mathematical expressions governing the coupled diffusion-limited/hydrodynamic-dissolution regime.

characteristics, the resulting concentration profile can be obtained,

$$\frac{C_s - C_o}{C_s - C} = \exp\left\{\frac{-\beta_2}{\alpha_2 k_s}\left[(\gamma - 2\alpha_2 k_s t)^{1/2} - \left[\gamma - 2\alpha_2 k_s\left(t - \frac{z}{v}\right)\right]^{1/2}\right]\right\}, \quad (16)$$

where β_2 and γ are lumped constants containing experimentally determined parameters.

The concentration profiles for each dissolution regime have now been determined. The final step toward modeling the release of phosphonate from a precipitation squeeze treatment is to describe how the porous media are discretized to improve model accuracy as well as to explain the transition from one dissolution regime to the next.

Simulation methodology

During the course of the precipitate release process, the precipitate surface area available for dissolution varies down the length of the porous medium, due, in large part, to the changing concentration driving force, $(C_s - C)$, as a function of position. In addition, the dissolution regime governing the release of HEDP may vary down the length of the porous media. To accurately account for these phenomena and effectively use the analytical concentration profiles to obtain elution curves, the porous media under study was discretized, as shown in Figure 9. Within each discrete section, $(C_s - C)$ is assumed constant, which is valid when the section lengths are small. By using the effluent concentration from the $(n-1)$ section as the inlet concentration to section n, the preceding analytical solutions can be used to obtain the concentration profile of the given section at each time step. The precipitate's characteristic radii and/or diffusion length are monitored as a function of time in each section so that within each discrete time step, the proper reaction conditions, that is, surface area/diffusion length, are used.

The transition from one release regime to another in the model was based on micromodel observations. After the initial HEDP solution in contact with the precipitate was eluted from the porous medium, the hydrodynamic dissolution of the long fibers began. When the radii of fibers became zero, the release regime was switched over to the coupled internal hydrodynamic/diffusion-controlled dissolution regime. As expected, not all sections were in the same dissolution regime at a given time due to the changing concentration driving force as a function of position. In the coupled external/internal hydrodynamic/diffusion-controlled dissolution regime for each section, the spherical cap and the length of the pore-throat plug receded simultaneously. With the spherical cap dissolving more rapidly than the plug itself, the tip of the plug flattened and continued to dissolve by diffusion until it reached a critical size, at which point the site broke and migrated from the system. This critical size was determined empirically from micromodel observations. After migration, the section was considered inert in that no more dissolution occurred.

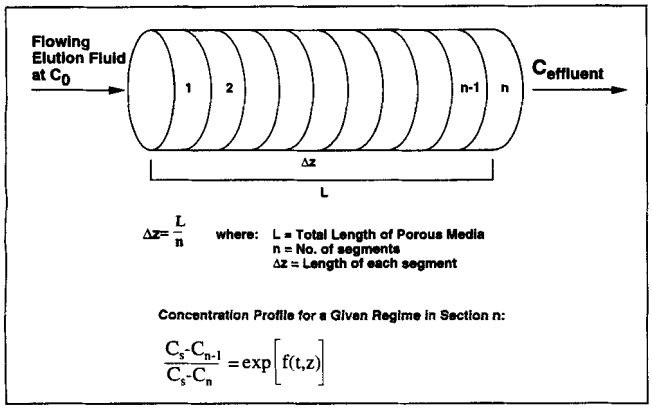

Figure 9. Discretization of porous media to model the precipitate release process.

1:1 Calcium-HEDP Model Results and Discussion

With the description of the mathematical model complete, the focus now becomes to evaluate how well the model describes the release of phosphonate from porous media. The elution curves described in this section simulate the release of a 1:1 calcium-HEDP precipitate from a micromodel. The parameters used for these simulations were either determined experimentally or recorded directly from micromodel experiments (averaged over many micromodels). The model contains no adjustable parameters. Table 1 shows the input parameter values used in each simulation, unless otherwise stated. The resulting simulated elution curves are discussed below.

Breakdown of simulated elution curves

The focus of this section is to determine how each release regime contributes to the shape of the simulated elution curve. A standard simulated elution curve is shown in Figure 10. This elution curve contains all of the features that were observed experimentally. The sharp initial decline (first 3–4

Table 1. Standard Input Parameter Values Used in Model Simulations

Description of Input Parameter	Parameter Value
Inlet phosphonate conc., C_o	0 ppm
Molar density of precipitate, ρ	0.00447 mol/cm^3
Equilibrium phosphonate conc., C_s	1,380 ppm
Flow rate of elution fluid, Q	0.05 cm^3/min
Pore vol. of micromodel, PV	0.043 cm^3
Init. radius of spindles, r_o	0.00025 cm
Diffusion coefficient, D	1.08E-05 cm^2/s
Kinematic viscosity, ν	0.01 cm^2/s
Total length of spindle, L	0.1405 cm
Fract. of spindle outside pore throat, f	0.68
No. of spindles in ppt. site, n	100
Site density, N/V	6,000 sites/cm^3
Avg. length of pore throat, L_{pt}	0.04496 cm
Time step used in simulations, t_s	120 s
No. of discretized sections, N_o	100
Init. radius of spherical particles, R_o	0.0030 cm

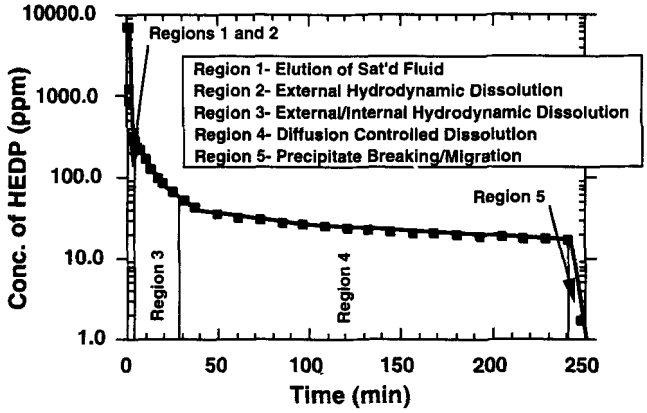

Figure 10. Contribution of each release regime to the overall shape of a simulated elution curve.

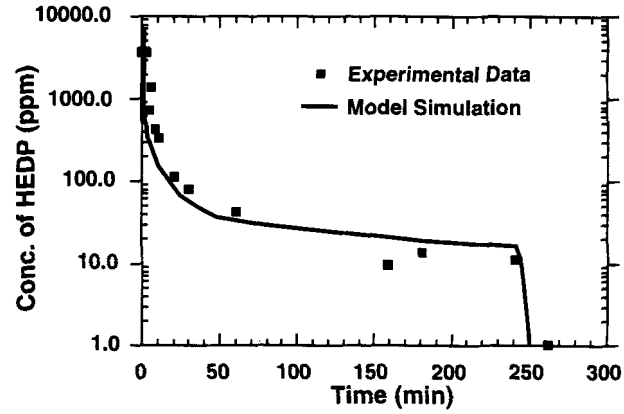

Figure 11. Comparison of simulated elution curve with a corresponding micromodel elution curve.

pore volumes) is followed by a more gradual decline and then by the flattening or long tailing of the elution curve. Finally, a final sharp decline is observed due to the migration/complete dissolution of precipitate sites.

Because each release regime governing the release process is known *a priori* throughout the simulation, one can determine how each release contributed to the shape of the curve. The first two release regimes, the release of saturated calcium-HEDP solution and the rapid hydrodynamic dissolution of long fibers extending into the pore bodies, lend themselves to high-effluent concentrations for a short period of time. A closer look at the first part of the elution curve reveals that an initial sharp decline in concentration occurs immediately following the first release regime and during the second release regime. Following the second release regime, the hydrodynamic dissolution of the spherical cap precipitate region in contact with free-flowing fluid begins (region 3), resulting in a gradual decline in the elution curve. This gradual decline, along with the fact that the effluent concentrations are lower than in the previous regimes is due, in large part, to the decrease in the precipitate's surface area available for hydrodynamic dissolution. The long tailing region of the elution curve (region 4) begins when the spherical cap has receded within the pore throat to the point where the diffusion of phosphonate from the precipitate surface (within the pore throat) to free-flowing fluid at the pore-throat entrance governs the rate of dissolution. This diffusion-limited dissolution dominates the release of phosphonate until the precipitate site reaches a critical size (dependent upon the flow rate and determined empirically) and breaks/migrates from the micromodel, resulting in the sharp, final decline of the effluent concentration, which constitutes the fifth release regime (see Figure 10).

Comparison of simulations with micromodel elution curves

Having defined the contribution of each release regime to the resulting simulated elution curve, we must now compare the shape and magnitude of a simulated elution curve with an actual elution curve. The input parameters (flow rate, site density, etc.) for these simulations were identical to the experimental micromodel conditions. The micromodel data were highly reproducible, showing small variations (within 5%) between experiments. The comparison between a simulated elution curve with an actual micromodel elution curve is shown in Figure 11. The shape and relative magnitudes of the two curves clearly indicate that the model (with no adjustable parameters) does an excellent job in describing the release of phosphonate from a micromodel as well as predict the time in which the phosphonate is exhausted from the model, that is, the squeeze lifetime. The slight discrepancies between the actual elution curve and the simulated elution curve can likely be attributed to the external migration of loose precipitate and the distribution of precipitate site properties (e.g., size) not accounted for in this version of the model. In porous media with severe microscopic and macroscopic heterogeneities (where the porous media and the precipitate sites would have a larger distribution of properties), the elution fluid-flow distribution and the precipitate surface area available for dissolution would be severely altered, likely affecting the local fluid properties (i.e., velocity, HEDP concentration) in contact with the precipitate sites. These changes in fluid properties, in turn, would impact the rate of precipitate dissolution and could increase the deviation between model and experimental elution curves. However, because the actual dissolution mechanisms remain intact, the model can be modified to account for such severe heterogeneities.

To examine the sensitivity of the model with respect to changing input parameters, one of the most important input parameters, the diffusion coefficient, was varied. The predictions are shown in Figure 12. As the diffusion coefficient is increased, the effluent concentrations increased only slightly, resulting in an upward shift in the elution curve and a smaller tailing region which, in turn, lends itself to shorter squeeze lifetimes.

Effect of flow rate on the phosphonate release from porous media

The effect of elution-fluid flow rate on the release of calcium-HEDP precipitates from porous media was studied to further test the ability of the model to simulate phosphonate release from a micromodel. Micromodel experiments were performed at three different flow rates (0.005, 0.05 and 0.5

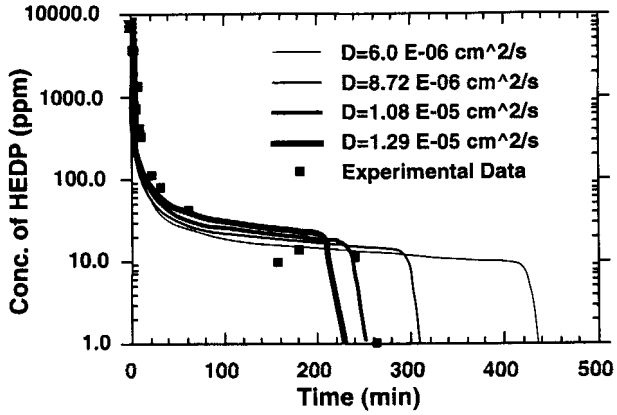

Figure 12. Sensitivity of the diffusion coefficient on the simulated elution curves.

cm^3/min), and the resulting elution curves are shown in Figure 13. One observes from this figure that as the flow rate is decreased, the effluent concentrations increase, resulting in a upward shift of the elution curve. This trend can be explained by the fact that although decreasing the flow rate decreased the local mass transfer from the precipitate surface to the bulk fluid (see mass-transfer correlations defined in the equations given earlier), the residence time with which the fluid was in contact with the precipitate was significantly increased and resulted in higher effluent concentrations. Similar trends were observed in ceramic coreflood experiments as well.

To predict how the elution-fluid flow rate affected the release of calcium-HEDP precipitate from a micromodel, model simulations were performed at the corresponding flow rates and the simulated elution curves are compared with the experimental curves in Figure 13. Using no adjustable parameters in these simulations, the model successfully predicted the experimental trends in flow rate and the magnitude of the effluent concentrations. The slight disparities between the model simulations and the experimental elution curves at each flow rate can again be attributed to the distribution of the precipitate-site properties and experimentally observed external precipitate migration.

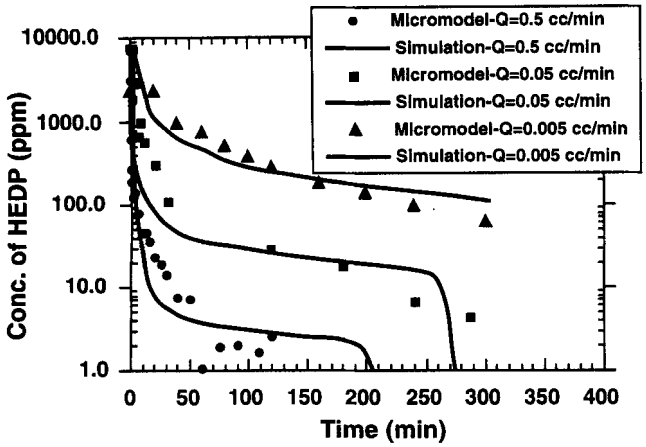

Figure 13. Effect of flow rate on the simulated and experimental elution curves (1:1 calcium-HEDP precipitate).

Modeling the Release of 2:1 Calcium-HEDP Precipitate

The first part of this study has focused on modeling the release of fibrous, 1:1 calcium-HEDP precipitate from porous media. The modeling efforts in this section, however, are focused on studying the release of a second precipitate, a 2:1 calcium-HEDP precipitate, from a porous medium. Past research showed that changing the conditions (pH, calcium/HEDP molar ratio) under which calcium and HEDP precipitated, resulted in a vastly different precipitate, one comprising rather insoluble spherical particles (Browning and Fogler, 1995b). Hence, the dissolution rate for the 2:1 precipitate is much slower than that for the 1:1 precipitate previously discussed. A typical elution curve for this precipitate is illustrated in Figure 14. For the 2:1 calcium-HEDP precipitate, the elution curve is divided into two distinct regions: (1) the initial flat region; and (2) the long tailing region. Note that this curve differs from the 1:1 calcium-HEDP elution curve in that the regions are more distinct. By comparing time-lapse photographs showing the release of this particular precipitate from a micromodel with the standard elution curve, the HEDP release mechanism in each region can be described as follows (see Figures 14 and 15):

Region 1. Release of saturated calcium-HEDP solution initially in contact with the precipitate.

Region 2. Slow, hydrodynamic dissolution of spherical particles (most likely mechanically trapped or bridged) in the porous media.

The micromodel photographs reveal that the release of 2:1 calcium-HEDP precipitate from porous media is dominated by hydrodynamic dissolution of spherical particles. There-

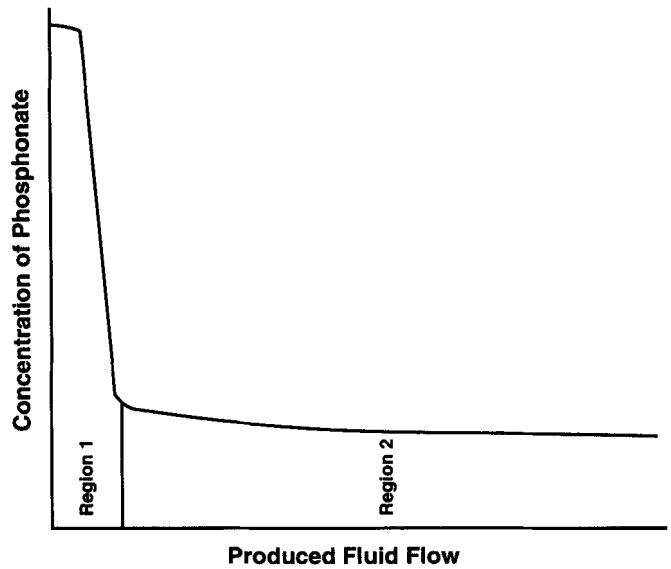

Figure 14. Breakdown of a typical elution curve resulting from the dissolution of a 2:1 calcium-HEDP precipitate in porous media.

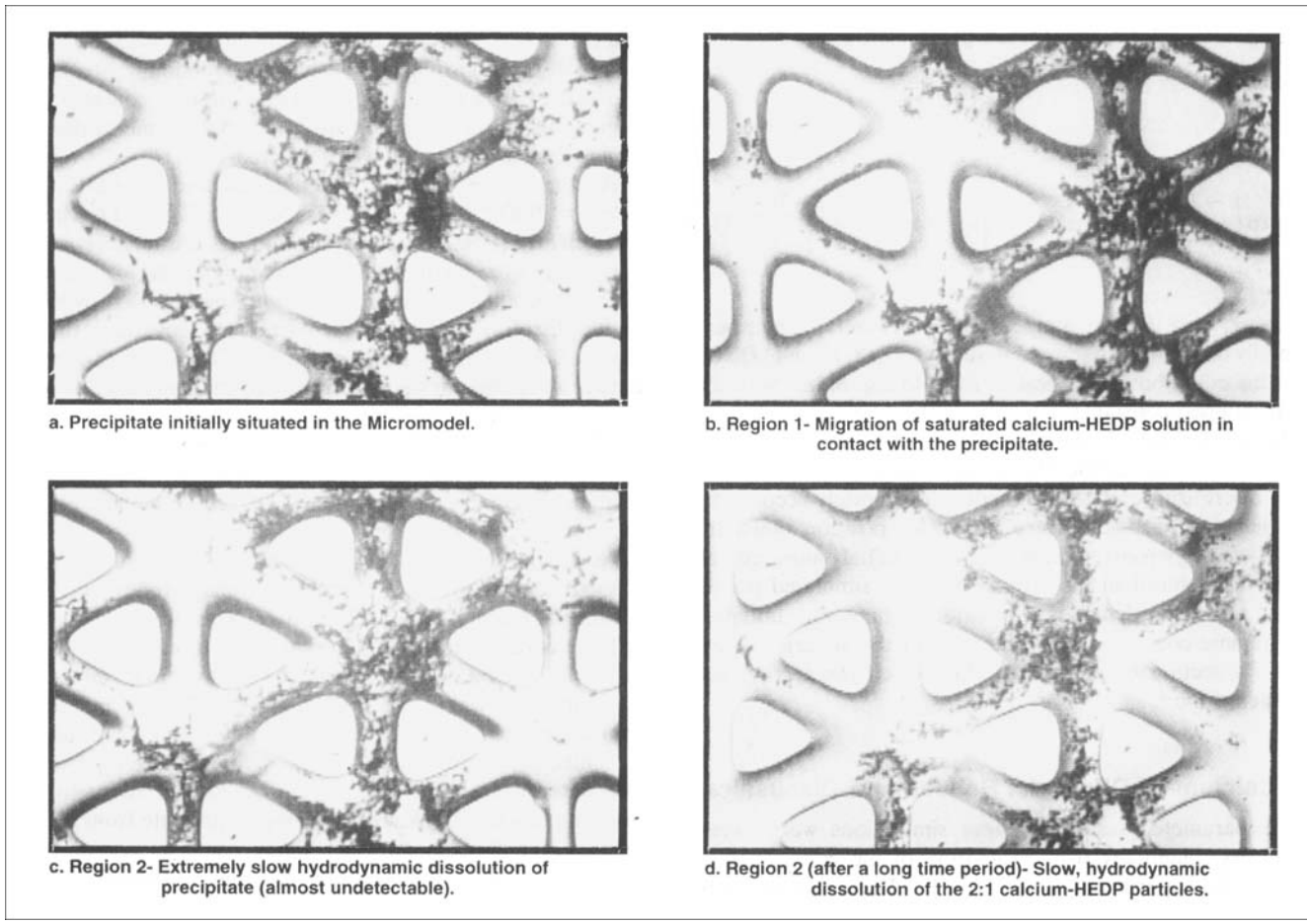

Figure 15. Different release regimes of 2:1 calcium-HEDP precipitate from a micromodel.

fore, this release process needs to be mathematically described.

The approach to model this dissolution regime is analogous to that described previously for the 1:1 calcium-HEDP precipitate. The physical geometry describing the dissolution of an individual spherical particle is shown in Figure 16. The mass-transfer coefficient for flow around a sphere is given by Eq. 7 (Cussler, 1993),

$$\frac{k_p d}{D} = 2.0 + \left(\frac{dv}{\nu}\right)^{1/2}\left(\frac{\nu}{D}\right)^{1/3}. \tag{7}$$

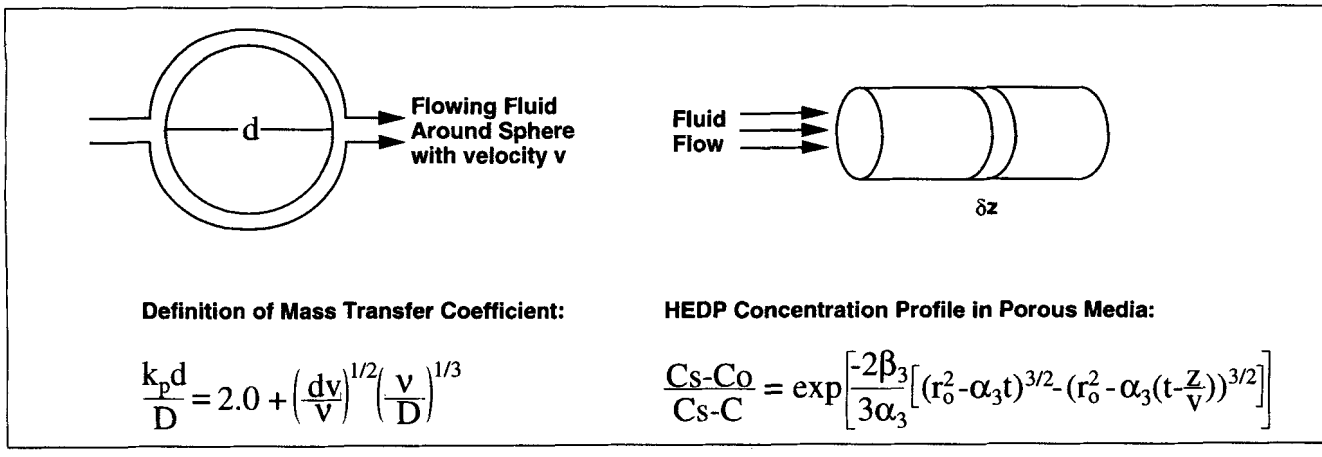

Figure 16. Physical geometry and mathematical expressions governing the hydrodynamic dissolution of spherical particles in porous media.

Coupled with Eqs. 1 and 2, the method of characteristics was used to obtain the concentration profile in this regime,

$$\frac{C_s - C_o}{C_s - C} = \exp\left\{\frac{-2\beta_3}{3\alpha_3}\left[(r_o^2 - \alpha_3 t)^{3/2} - \left[r_o^2 - \alpha_3\left(t - \frac{z}{v}\right)\right]^{3/2}\right]\right\} \quad (17)$$

where α_3 and β_3 are lumped constants containing experimentally determined parameters such as D, N/V, and ρ. Note that this equation is identical in form to Eq. 8, but with different lumped constants.

Having defined the concentration profile in the hydrodynamic dissolution regime, the simulations were performed by again discretizing the porous media to accurately account for the changing particle surface area with position down the length of the porous medium. Once the initial saturated calcium-HEDP solution was flushed from the simulated porous media, the hydrodynamic dissolution regime was initiated. This regime continued until the radii of the spherical particles in a section became zero, after which the section was considered inert.

2:1 Calcium-HEDP Model Results and Discussion

The parameters used for these simulations were determined experimentally from evaluation of the corresponding micromodel experiments (see Table 1). The resulting simulated elution curves are discussed below.

Evaluation of a simulated 2:1 elution curve

A simulated elution curve describing the release of a 2:1 calcium-HEDP precipitate is shown in Figure 17. This simulated curve, which contains all the features that were observed experimentally in micromodel experiments, can be bisected into two distinct regions. In the first region, the elution of saturated calcium-HEDP solution from the simulation

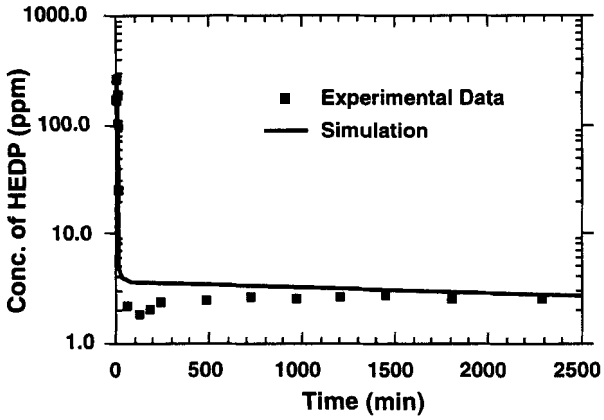

Figure 17. Comparison of simulated vs. experimental elution curves describing the release of 2:1 precipitate from porous media.

matrix dominates the release of HEDP. Following this regime, the release of phosphonate was simulated by slow, hydrodynamic dissolution of spherical particles randomly situated in the matrix. The sharp decline in the effluent concentration occurs during the transition from the first regime to the second regime as dispersion was neglected.

A comparison between experimental and theoretical 2:1 calcium-HEDP elution curves is shown in Figure 17. The results clearly show that the simulated 2:1 elution curve is in very good agreement with the micromodel elution curve in both shape and magnitude, solidifying the fact that hydrodynamic dissolution of spherical particles is governing the release of HEDP from the micromodel. The slight differences between the two curves is likely due to the fact that all of the spherical particles are not uniform in size or are not uniformly distributed throughout the micromodel. Additional simulations have indicated that accounting for these nonuniformities improves the agreement between model and experimental results slightly.

As previously noted, the 2:1 calcium-HEDP elution curve is significantly different (in shape and magnitude) from that for the 1:1 calcium-HEDP precipitate. This difference is due, in large part, to the vastly different dissolution characteristics of each precipitate that result from dissimilar molecular structures (Browning and Fogler, 1995b). The 2:1 precipitate is more insoluble than the 1:1 precipitate (the HEDP solubility limits, C_s, for the 2:1 and 1:1 precipitates were experimentally determined to be 12.2 ppm and 1,380 ppm, respectively), resulting in a steady, slow release of phosphonate from porous media. This phenomenon was highly visible in consolidated porous media as well (Browning and Fogler, 1995a).

Effect of flow rate on the release of 2:1 calcium-HEDP

A micromodel experiment with 2:1 calcium-HEDP precipitate was performed at an initial flow rate of 0.05 cm^3/min where after approximately 47 h, the flow rate was reduced to 0.005 cm^3/min for a period of time, after which the flow rate was returned to 0.05 cm^3/min. The resulting elution curve is shown in Figure 18. As shown in the resulting elution curve, this step decrease in the flow rate resulted in a step increase in the effluent concentration. This increase is due to an increase in the contact time between the elution fluid and the precipitate situated in the micromodel. Once the flow rate was increased to its original value, the concentration decreased accordingly. A model prediction of this micromodel experiment is also shown in Figure 18. As was the case in the micromodel curve, it is apparent that a step decrease in the flow rate resulted in a step increase in the effluent concentration. To further illustrate the effect of flow rate on the elution curve, model simulations were performed at flow rates of 0.5, 0.05 and 0.005 cm^3/min, respectively, and the results are shown in Figure 19. This figure reconfirms the fact that decreasing the flow rate results in an increase in the effluent concentration, and shows how the 2:1 model can be used as a predictive tool in studying the effects of system parameters on the release of 2:1 precipitate from a micromodel.

Implications of Mathematical Modeling

Micromodel experiments showed that the release of 1:1 calcium-HEDP precipitate from porous media occurs in five

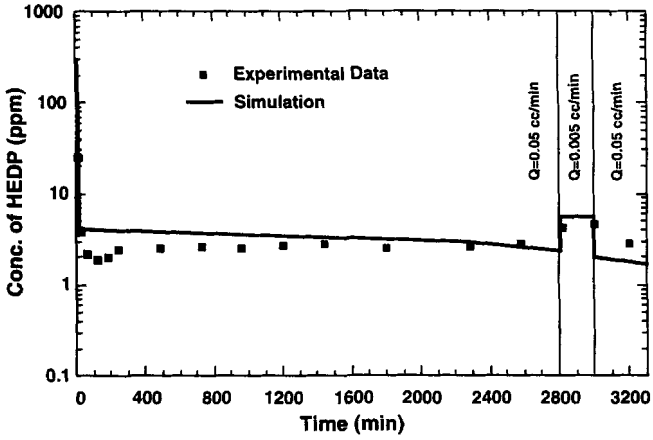

Figure 18. Effect of flow rate on the simulated and experimental elution curves for a 2:1 precipitate.

distinct release regimes, while the release of 2:1 calcium-HEDP precipitate is governed by two distinct release regimes. This article has focused on describing a continuum mathematical model that incorporates each of these distinct release regimes to simulate the release of different calcium-HEDP precipitates from a micromodel. This model is unique in that it used a fundamental scientific basis (with no adjustable parameters) to effectively predict how calcium-HEDP precipitates behave in porous media during a precipitation squeeze treatment. The pore-level approach taken to model the calcium-HEDP precipitate release made it feasible to account for often overlooked phenomena such as definitive dissolution mechanisms or precipitate morphologies. By mathematically describing the well-defined pore-level dissolution mechanisms, it becomes possible to elucidate which factors govern the calcium-HEDP release process and to predict how changing the system conditions affect these factors and the subsequent release process. This information, in turn, can be effectively used to enhance the design of precipitation squeeze treatments. In addition to simulating the release of phosphate precipitates from porous media, this model can be extended to other related applications, including (1) the dissolution of other precipitates from porous media; (2) the release of nonaqueous phase liquids (NAPLs) from porous media (Geller and Hunt, 1993; Miller et al., 1990); and (3) the release of phosphonates in other industrial processes where phosphonate treatments are prominent, for example, in cooling water towers. Finally, the framework of this model can be used as a basis for more sophisticated models, such as physically representative network models, that can account for large microscopic and macroscopic heterogeneities as well as permeability changes due to precipitate formation and dissolution in porous media.

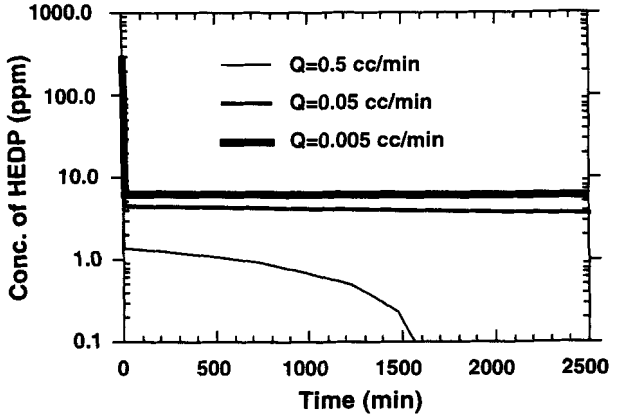

Figure 19. Simulations showing the effect of flow rate on the release of a 2:1 calcium-HEDP precipitate from porous media.

Conclusions

- The elution of a fibrous 1:1 calcium-HEDP precipitate from a micromodel indicated that five distinct release regimes govern the release of HEDP from porous media, with the long tailing region being dominated by the diffusion-limited dissolution of compacted precipitate sites situated in pore throats. A continuum mathematical model was developed to simulate this release process by mathematically describing each of the distinct release regimes and defining conditions under which the transition between release regimes occurs.
- A comparison between micromodel elution curves and simulated elution curves resulting from the release of 1:1 calcium-HEDP precipitate showed excellent agreement in both shape and magnitude. A sensitivity analysis performed by varying the diffusion coefficient indicated that an increase in the diffusion coefficient magnitude marginally increased the rate at which HEDP was released.
- The 1:1 calcium-HEDP model simulations performed at different flow rates showed good agreement with micromodel experiments and reconfirmed the fact that an increase in the flow rate increases the effluent concentration, resulting in an upward shift of the resulting elution curve.
- A mathematical model was also developed to simulate the release of highly insoluble 2:1 calcium-HEDP spherical particles from a micromodel. The elution curve was modeled as being dominated by the elution of saturated calcium-HEDP solution from porous media followed by the hydrodynamic dissolution of spherical particles situated throughout the simulation matrix. The shape of the elution curve was formed by an initial sharp decline in concentration, followed by an extremely long tailing region.
- A comparison of model and experimental elution curves showed that the model was accurately simulating the release of a 2:1 calcium-HEDP precipitate from a micromodel. In addition, simulations performed at different flow rates showed that decreasing the flow rate increased the effluent concentrations, reinforcing results previously observed in micromodel and coreflood experiments.

Notation

k_i = mass-transfer coefficient for ith reaction regime, cm/s
v = linear velocity of elution fluid, cm/s
r = radius of characteristic precipitate geometry at any time, cm
r_o = initial radius of characteristic precipitate geometry, cm
L_o = initial length of a precipitate compaction region, cm
C_{eff} = effluent phosphonate concentration from porous media, mg/L
r'' = reaction rate per unit surface area, mol/cm^2·s

Literature Cited

Atkinson, L. M., M. D. Yuan, K. S. Sorbie, and A. C. Todd, "The Modelling of Adsorption and Precipitation Scale Inhibitor Squeeze Treatments in North Sea Fields," Oilfield Chemistry Symp., New Orleans, LA (1993).

Berkshire, D. C., J. B. Lawson, and E. A. Richardson, "Treating Wells With Self-Precipitating Scale Inhibitor," U.S. Patent No. 4,357,248 (1982).

Bird, R. B., W. E. Stewart, and E. N. Lightfoot, *Transport Phenomena*, Wiley, New York (1960).

Browning, F. H., and H. S. Fogler, "Precipitation and Dissolution of Calcium-Phosphonates for the Enhancement of Squeeze Lifetimes," *SPE Prod. Facil.*, (1995a).

Browning, F. H., and H. S. Fogler, "The Effect of Synthesis Parameters on the Resulting Properties of Calcium-Phosphonate Precipitates," *Langmuir*, (1995b).

Carlberg, B. L., "Scale Inhibitor Precipitation Squeeze for Non-Carbonate Reservoirs," Production Technology Symp., Lubbock, TX (1987).

Ciba-Geigy Corporation, "Bellasol S29-Phosphorous-Containing Polymeric Scale Inhibitor," Hawthorne, NY (1989).

Cussler, E. L., *Diffusion: Mass Transfer in Fluid Systems*, Cambridge Univ. Press, New York (1984).

Geller, J. T., and J. R. Hunt, "Mass Transfer From Nonaqueous Phase Organic Liquids in Water-Saturated Porous Media," *Water Resour. Res.*, **28**(4), 833 (1993).

Hach Company Rep., "Phosphonates," Hach Chemical Co., Loveland, CO (1980).

Hoefner, M. L., and H. S. Fogler, "Pore Evolution and Channel Formation during Flow and Reaction in Porous Media," *AIChE J.*, **34**, 45 (1988).

Kan, A. T., J. E. Oddo, and M. B. Tomson, "Acid/Base and Metal Complex Solution Chemistry of the Polyphosphonate DTPMP vs. Temperature and Ionic Strength," *Langmuir*, **10**, 1442 (1994).

Miller, C. T., M. M. Poirier-McNeill, and A. S. Mayer, "Dissolution of Trapped Nonaqueous Phase Liquids: Mass Transfer Characteristics," *Water. Resour. Res.*, **26**(11), 2783 (1990).

Mohanty, R., S. Bhandarkar, and J. Estrin, "Kinetics of Nucleation from Aqueous Solution," *AIChE J.*, **36**(10) (1990).

Monsanto Tech. Bull., "Dequest 2060 Phosphonate," Publ. WT-8601 (1986a).

Monsanto Tech. Bull., "Dequest 2010 Phosphonate," Publ. 9024 (1986b).

Nancollas, G., "The Growth of Crystals in Solution," *Adv. Colloid Interf. Sci.*, **10**, 215 (1979).

Rege, S. D., and H. S. Fogler, "Competition Among Flow, Dissolution, and Precipitation in Porous Media," *AIChE J.*, **35**(7), 1177 (1989).

Rhee, H. K., R. Aris, and N. R. Amundson, *First Order Partial Differential Equations*, Prentice Hall, Englewood Cliffs, NJ (1986).

Walsh, M. P., S. L. Bryant, R. S. Schechter, and L. W. Lake, "Precipitation and Dissolution of Solids Attending Flow through Porous Media," *AIChE J.*, **30**(2), 317 (1984).

Walton, A., *The Formation and Properties of Precipitates*, Interscience, New York (1967).

Yuan, M. D., K. S. Sorbie, and A. C. Todd, "A Near-Well Simulator for Modelling Scale Inhibitor Squeeze Treatments," NACE Corrosion 92, Nashville, TN (1992).

Manuscript received Dec. 11, 1995, and revision received Mar. 18, 1996.